Available online at www.sciencedirect.com

SCIENCE DIRECT®

Geomorphology 64 (2005) 299–314

GEOMORPHOLOGY

www.elsevier.com/locate/geomorph

The Amspoort Silts, northern Namib desert (Namibia): formation, age and palaeoclimatic evidence of river-end deposits

B. Eitel[a,*], A. Kadereit[b], W.D. Blümel[c], K. Hüser[d], B. Kromer[e]

[a]*Institute of Geography, University of Heidelberg, INF 348, 69120 Heidelberg, Germany*
[b]*Forschungsstelle Archäometrie der Heidelberger Akademie der Wissenschaften am Max-Planck-Institut für Kernphysik, Saupfercheckweg 1, 69117 Heidelberg, Germany*
[c]*Institute of Geography, University of Stuttgart, Azenbergstr. 12, 70174 Stuttgart, Germany*
[d]*Department of Geosciences, Universität Bayreuth, Universitätsstr. 30, 95447 Bayreuth*
[e]*Forschungsstelle Radiometrie der Heidelberger Akademie der Wissenschaften, Institute of Environmental Physics, University of Heidelberg, INF 248, 69120 Heidelberg, Germany*

Received 2 February 2004; received in revised form 17 June 2004; accepted 13 July 2004
Available online 21 August 2004

Abstract

Detailed geomorphological and chronological investigations of the NW-Namibian Amspoort Silt formation show that the sediments are typical river-end deposits. This type of endoreic sediment, occuring only in desert margin areas, provides valuable information about the palaeo-environment. In the Hoanib valley, the fine-grained deposits have buried riverine trees. Radiocarbon dating of the wood and luminescence dating of the sediments allow a detailed reconstruction of the aggradation processes. Accumulation started ~10 km downstream of Amspoort around the beginning of the 15th century and ended in the 19th century, some kilometres upstream of Amspoort. This upstream shift of sedimentation during the Little Ice Age was caused by gradually decreasing runoff resulting from aridification of the upper part of the Hoanib river catchment lying east of the Namib desert margin ≥1.200 m a.s.l.

The Amspoort Silt terrace is evidence of palaeo-hydrological fluctuations in NW-Namibia. At present, the Hoanib river erodes deeply into the silty deposits, indicating that NW-Namibia receives more monsoonal rainfall today than during the Little Ice Age. However, this contradicts the hypothesis of a (continual) natural aridification of NW-Namibia (Damaraland, Kaokoveld) since the mid-19th century in the course of global climatic change. Rather, deposition and erosion of the Amspoort Silts indicate that landscape degradation in NW-Namibia is primarily anthropogenically induced and most probably not accelerated by a decrease in precipitation.

Keywords: Namibia; Amspoort Silts; River-end deposits; Little Ice Age; Luminescence dating; Radiocarbon dating

* Corresponding author. Tel.: +49 6221 544543.
E-mail address: Bernhard.Eitel@urz.uni-heidelberg.de (B. Eitel).

0169-555X/$ - see front matter © 2004 Elsevier B.V. All rights reserved.
doi:10.1016/j.geomorph.2004.07.006

1. Introduction

On the eastern margin of the Namib Desert (Namibia), fine-grained, mainly silty and partly sandy or clayey deposits are common along ephemeral rivers flowing through a sequence of narrow incised valleys and open tectonic basins (Rust, 1987, 1989, 1999; Rust and Vogel, 1988). The rivers run from the semiarid highlands of northwestern Namibia down to the hyperarid Namib coastal desert. During the last decade, research on silty fluvial deposits in desert margin areas has been intensified due to IGCP 349 activities on desert margins, IGCP 413 projects on dryland environmental changes, and by the possibility of dating the sediments by luminescence techniques [thermally stimulated luminescence (TL) dating, optically stimulated luminescence (OSL) dating]. For Namibia, all published data show that the sediments formed within the past 45 ka (see compiled data in Eitel et al., 2002a; Srivastava et al., 2004a,in press).

Although the deposits contain thin layers of fluvial sands, they predominantly consist of—more or less—clayey silts with loess-like particle characteristics. For this reason, most of the time they are called 'river *silt* deposits'. Since the 1970s, the fine-grained deposits have been studied geomorphologically and palaeoclimatically, but their interpretations have proved controversial. Because of their fine-grained character, the deposits have sometimes been interpreted as ancient lake deposits (Rust and Wieneke, 1974), which in some cases were proposed to have been caused by dune damming (Marker, 1977). However, more recently the fluvial genesis of the sediments was recognized. They have been (re)interpreted either as sequences of flash flood or slackwater materials (Heine et al., 2000; Heine and Heine, 2002; Heine, 2004; Srivastava et al., 2004a,in press) or as river-end deposits (Eitel et al., 2001, 2002a; Rust, 1999). Whereas slackwater deposits are attributed to high-energy flash floods (Zawada, 1997), river-end deposits are created by low-energy runoff resulting from endoreic discharges (Eitel et al., 2001). River-end deposits are due to seasonal or decadal fluctuations of river discharges causing fluvial sedimentation not only at one final position but allowing for shifts of several kilometres in up- and downstream directions within a valley section. This distinguishes river-end deposits from sebkha or lake deposits that indicate stationary sedimentary environments. Apart from this, variations in discharge lead to varying proportions of sand, silt and clay within the silty river-end deposits, in contrast to more homogeneous still water sediments.

The differing interpretations of the sediments have led to contrasting palaeo-climatic conclusions. Whereas slackwater deposits are caused by heavy rainfall in the catchments of the rivers, river-end deposits are geomorphological markers of rather dry conditions upstream. The aggradation of river-end deposits is still not well understood (compare, e.g., discussions of Rust, 1999 and Heine, 2004). The present study of the Amspoort Silt formation is a valuable contribution to the understanding of river-end deposits and their palaeoclimatical interpretation, as it combines detailed sedimentological and geomorphological investigations with a radiocarbon- and luminescence-based chronometry.

2. Geographical setting

Along the Hoanib river (northwestern Namibia) and both its upper tributaries, the Nguravai-Aap and the Ombonde rivers, silty deposits are common within the epigenetically incised valleys and tectonic basins (Spönemann and Brunotte, 2002). During the austral summer when precipitation falls due to monsoonal thunderstorms, the Hoanib river flows down from the western Etosha rim (~1200 m a.s.l.; ~350-mm mean annual rainfall) to the hyperarid northern Namib desert. Ten to 20 km east of the coast, the Skeleton Coast Erg hinders the river from discharging into the Atlantic Ocean (Fig. 1). Occasionally, the Hoanib catchment receives enough rain for the river to break through the sand field in catastrophic events.

At Amspoort, approximately 300 m a.s.l. and 40 km east of the coast, the sediments fill the Hoanib valley up to more than 12 m. Over a length of about 20 km, the deposits have buried riverine trees, which rooted in basal fluvial sands some decimeters above the bedrock of Precambrian Damara schists. The site was first described in detail by Rust (1999), Vogel (1989) and Vogel and Rust (1990). At present, erosion

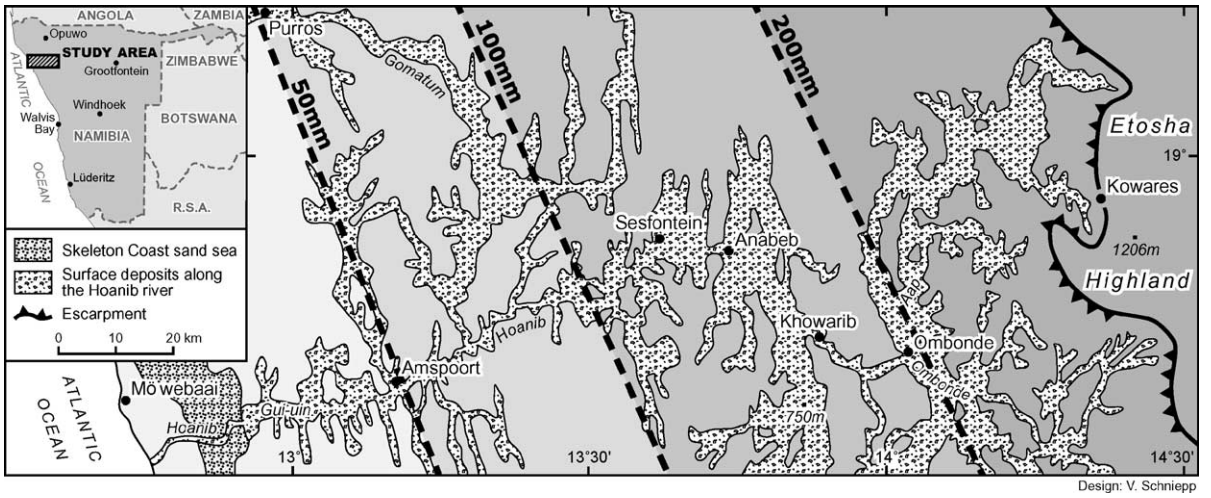

Fig. 1. Surface deposits along the Hoanib river in northwestern Namibia. The study area is ~40 km east of the coast near Amspoort, where the fine-grained deposits form the Amspoort Silts within the narrow lower Hoanib valley.

processes are removing the Amspoort Silts and thus forming a 50–200 m broad river channel and a prominent terrace (Fig. 2), and are thereby reexposing the fossilized wood. The exposed walls of the silt terrace show that the trees were embedded upright (Fig. 3). From this important observation, Vogel and

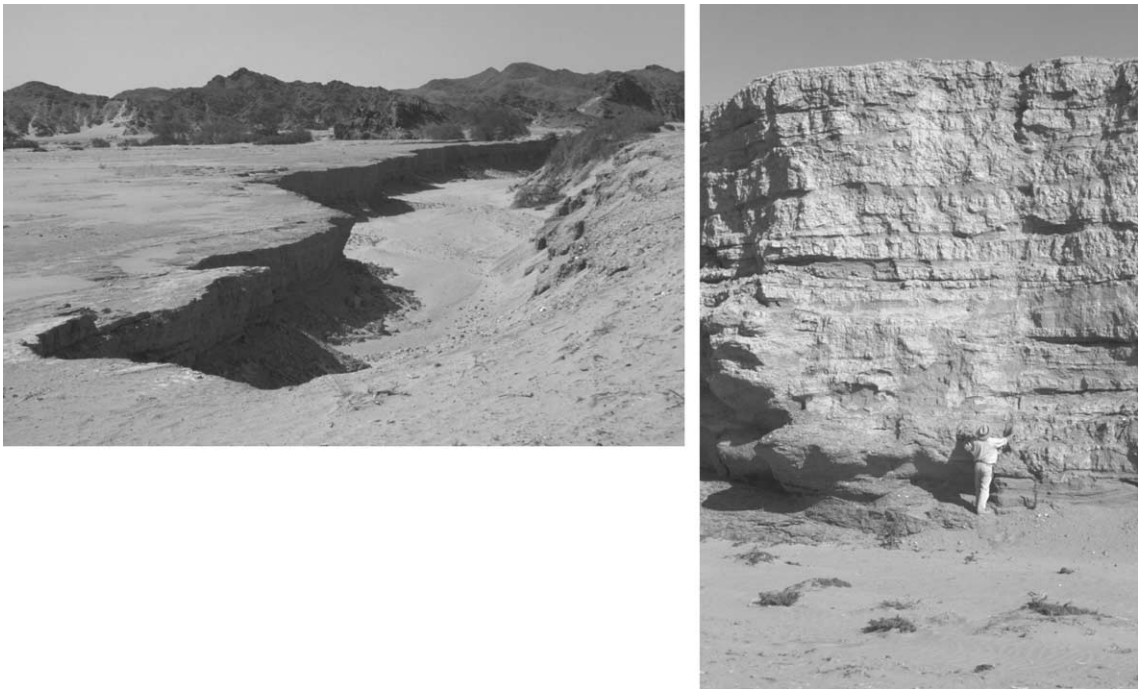

Fig. 2. The Amspoort Silts in a central valley section. Left side: Overview over the Amspoort silt deposits with a tributary erosion channel in the foreground. The Hoanib river running from the left to right side is indicated by green riverine trees. Right side: The deposits are dominated by well-laminated fluvial silts with intercalated thin layers of sand. Note the lack of coarse-grained materials, which indicates sedimentation by low-energy flows.

Fig. 3. The silt terrace at locality 3, some kilometres upstream of Amspoort. The photos show a buried in situ tree (left side) of an ancient riverine forest that is now being reexposed by river erosion (right side). Height of the terrace is ~3 m.

Rust (1990) and Rust (1999) excluded high-energy slackwater deposition at Amspoort. Instead, they argued that the Hoanib river deposited silty river-end sediments while ending here endoreically during a drier phase in the past. This is confirmed by the laminar character of the silts indicating a sequence of run-off terminations, by the occurrence of the silty deposits not only in backflood positions (i.e., at tributary mouths) but also in central parts of the main valley, and finally by the fact that the sediments have been deposited only in a spatially well defined part of the Hoanib valley. Backfloods due to high-energy runoff, however, should be distributed over the whole length of the river course.

The association of buried trees and fine-grained silty sediments offers the possibility to use two independent dating methods. Therefore, in this study, radiocarbon dating of the wood and OSL dating of the sediments are applied to determine the age of the deposits, to reveal details of the course of the aggradation history and to interpret the Amspoort Silt terrace palaeo-climatically.

3. Methods

Samples were taken at three sites where the river dissects the Amspoort Silts, naturally exposing the fine-grained deposits:

- locality 1: downstream of Amspoort West of the Skeleton Coast Park border (GPS coordinates: 19°22′ 58″ S/13°02′ 57″ E),
- locality 2: at Amspoort itself (GPS coordinates: 19°21′ 44″ S/13°08′ 24″ E) and
- locality 3: upstream of Amspoort (GPS coordinates: 19°20′ 25″ S/13°11′ 23″ E).

3.1. Sedimentology

Sediment characteristics were determined at all three locations. Sediment colour was specified using the Munsell Soil Color Chart and carbonate content was measured with a Scheibler apparatus. Particle size distribution was investigated after treatment with H_2O_2 and HCl, by sieving the grain size fraction <2

mm and separating the silt and clay fractions applying the Köhn/Köttgen method (Kretzschmar, 1996). Heavy mineral identification of the fraction 0.063–0.2 mm in diameter, separated in an 80% solution of sodium polytungstate (density 2.8), was carried out using a petrographic microscope (Boenigk, 1983). Clay fractions were prepared by sedimentation in water. Oriented aggregates on glass targets that were either air-dried, glycollated or heated to 550 °C were analysed by X-ray diffraction (Velde, 1995).

3.2. Chronometry

3.2.1. ^{14}C dating

For radiocarbon dating two samples were taken between localities 1 and 2 (HD 22152) and at locality 3 (HD 22469) (Table 1, see Fig. 6). Both wood samples were collected from upright standing buried trees rooted in fluvial sands close to the bedrock base. Driftwood was not collected in order to avoid overestimating the age by using possibly reworked old wood. Sample HD 22152 originates from a twig of a fossil tree 1.2 m b.g.l. At locality 3, wood was sampled 0.5 m b.g.l. from a branch near the top of another in situ tree (cf. Fig. 3). Thus, the radiocarbon ages should represent dates from the final life period of the buried trees. It is possible that trees continued to grow in their upper canopy part, while embedding of the lower trunk part had already begun. Thus, the radiocarbon ages do not necessarily represent maximum ages for the oldest basal sediments. The ^{14}C data were calibrated following Stuiver et al. (1998).

Additionally, already published ^{14}C data from the area (Rust, 1999) were included in this study. These data, too, were gained from in situ buried trees which once grew in the basal fluvial sediments underlying the Amspoort Silt deposits. In order to allow for data comparison (Table 1, see Fig. 6) the conventional ^{14}C data produced in the Pretoria laboratory were also calibrated according to Stuiver et al. (1998).

Table 1
Results of the radiometric age determinations of the wood samples from the Amspoort study area (Hoanib valley)

Lab. No.	$^{14}C_{conv.}$ aBP	$\delta^{13}C$	$^{14}C_{cal.}$ AD 1σ	$^{14}C_{cal.}$ AD 2σ
Pta-3880	350±40	–	1480–1530, 1560–1640	1540–1640
Pta-4546	460±40	–	1415–1470	1400–1510 1600–1620
Pta-4547	280±45	–	1520–1600, 1620–1670	1480–1680 1770–1800
Pta-4548	330±40	–	1490–1640	1460–1650
Pta-7356	195±20	–	1660–1680, 1760–1810, 1930–1950	1650–1690 1730–1810 1930–1950
Hd-22152	154 ±18	−24.6	1670–1690, 1730–1780, 1800–1810, 1920–1940	1660–1700 1720–1820 1830–1880 1910–1960
Hd-22469	402±18	−24.5	1448–1478	1430–1500 1600–1620

3.2.2. OSL dating

Samples for luminescence dating were collected at all three localities (see Figs. 5, 6). From a total of seven samples, it was possible to extract coarse-grain (125–212 μm) quartz separates. At locality 1 the central silty deposits (HDS-1262, 2.6 m b.g.l.) and the aeolean sand, covering the fluvial deposits (HDS-1260, 0.3 m b.g.l.), were sampled. At locality 2, one sample was collected from the sandy silt complex intercalated between the lower and upper silty complexes (HDS-1267, 7.0 m b.g.l) and two samples were taken from the sand layer on top of the upper silty complex (HDS-1265, 1.5 m b.g.l and HDS-1264, 0.4 m b.g.l.). At locality 3, samples were gained from the basal fluvial sands covering the bedrock (HDS-1269, 2.3 m b.g.l.) and the sandy silt complex (HDS-1270, 0.4 m b.g.l.) at the top of the sequence.

Samples were taken from the exposed river terrace walls in lightproof steel cylinders (∅55 mm). In the luminescence dark laboratory the outer ~1 cm of the samples were removed and retained both for water content and dose-rate determinations. The nonlight-affected material from the interior used for luminescence analyses was handled under extremely subdued red light (Siemens LS5421-Q diodes plus Hoya R62 glass filter, Schilles, 1998). The 125–212 μm fraction from the retained sediment was derived by wet sieving. Organic and carbonate content was removed by repeatedly adding of H_2O_2 (10% and 30%) and CH_3COOH (20%). Quartz was gained by mineral separation in lithium polytungstate (densities ≤2.74 and ≥2.63 g cm^{-3}). Quartz separates were kept for 45 min in HF (40%) while occasionally stirring the fluid to etch off the outer rim (~20 μm) of the quartz grains possibly affected by external α-radiation. In order remove any residual fluorine compounds the separates

were washed in HCl (10%) and demineralised H_2O before the 90- to ~170-μm grain fraction was finally retrieved by dry sieving using a 90-μm mesh.

The quartz separates were mounted on steel cups (∅~10 mm) using silicon spray for adhesion. Since small aliquots with a restricted number of grains make it possible to test the sediment samples for insufficient, differential bleaching (Olley et al., 1998, 1999), aliquots containing 200–500 grains, as suggested by Fuchs and Wagner (2003), were prepared.

Luminescence dating was carried out using a Risø TL/OSL-reader DA15 (Bøtter-Jensen, 1997), which is equipped with a ring of 41 blue NISHIA NSPB-500 LEDs plus Schott GG-420 edge filter (470Δ20 nm) for blue stimulated (B-OSL) analyses, a photomultiplier EMI 9235 QA for signal detection and a calibrated $^{91}Sr/^{89}Y$ β-source (~5.1 Gy min^{-1}) for sample irradiation. For luminescence analyses a B-OSL single aliquot regenerative (SAR) procedure was applied (Murray and Wintle, 2000). Optical stimulation was carried out for 20 s at 125 °C (90% diode power) while the UV component was detected using U-340 Hoya glass filters (3×2.5 mm each). Four regeneration dose points were distributed at ~0.4/0.7/1.3/1.6 times of the expected D_E, before the lowest dose point was repeated once and finally a zero-dose point measured. A test dose of 5 s (~0.4 Gy) or 1 s (~0.1 Gy) (sample HDS-1260 only), respectively, was given after the study of the natural luminescence signal and the luminescence signals of each regeneration dose point in order to correct for sensitivity changes via the size of the related OSL signal. As in the temperature range of 220–300 °C no dependency on preheat temperature was discernable (Fig. 4) a preheat of 10 s at 260 °C was applied, while the cut heat (i.e., the preheat during the test dose subcycles) was held for 10 s at 160 °C. In order to test for possible feldspar contamination, finally each aliquot was administered the highest regeneration dose for a second time followed by an IR-stimulated readout for 20 s at room temperature. 32 aliquots were measured of each sample. For D_E-value determination, the integral of the first 0.4 s of the B-OSL shinedown was used, while the late light integral >16 s was taken for background subtraction.

Additionally, a set of 16 aliquots of each sample was bleached for 3 h under a Dr. Hönle SOL2 solar simulator. Sample holders were positioned on a water-cooled copper plate (~18 °C) and covered with a non-UV-transmitting UVILEX glass filter. The artificially

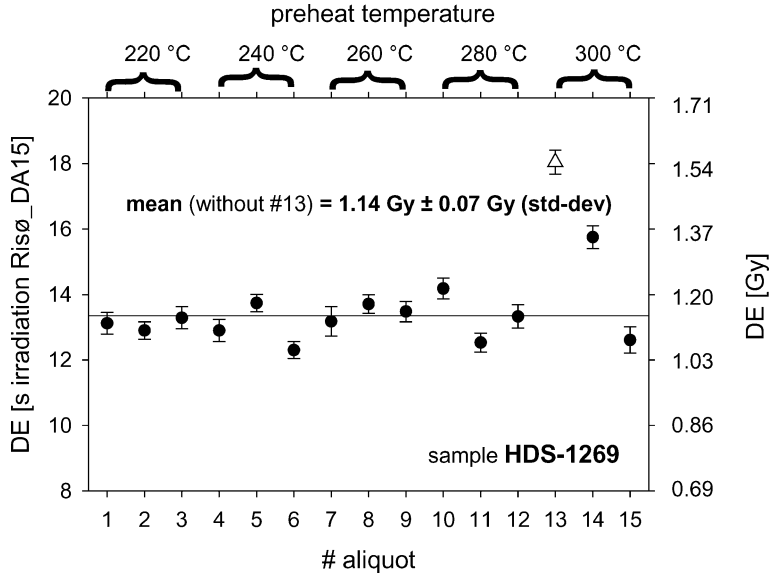

Fig. 4. Preheat test for sample HDS-1269. Altogether 15 small aliquots with latent natural luminescence signals were used for a preheat test with temperatures varying from 220 to 300 °C (five temperature steps, three aliquots each, preheat duration 10 s). D_E determination followed the SAR protocoll as described in the text above. D_E results show no dependency on preheat temperature. (Aliquot #13 (white triangle signature) shows a bad recycling ratio (>10%) of the lowest applied dose point of 1.21 and would therefore be excluded from the data set.)

(well) bleached samples were then given a β-laboratory dose the size of which corresponds to the mean D_E-value of the natural sample. The laboratory dose was then recovered using the same B-OSL SAR protocol as for the corresponding natural sample.

Dose rate determination is based on low-level γ-spectrometry, which allows the detection of possible radioactive disequilibrium in the ^{238}U-chain. Dose rates are additionally controlled by the use of α- and β-counts. The contribution of the cosmic radiation is calculated according to Prescott and Hutton (1998). The measured ratios of wet to dry sample weights δ range between 1.01 and 1.04. For effective doserate calculation, a uniform value of $\delta=1.05\pm0.05$ was used. Error determination follows Gaussian error propagation law and OSL ages are quoted on the 1-σ confidence level.

4. Results

4.1. Sedimentology

The grain size analyses show that all samples from the Amspoort Silt terrace lack coarse particles of >2 mm in diameter (Fig. 5). The silty deposits are well laminated and show no postsedimentary diagenesis. The silty units alternate with sandy layers, thus indicating varying velocities of the ancient runoff. Therefore, the 'Amspoort Silts' are strictly speaking not mere silts but cover a grain size spectrum from clayey silt to sand.

The colours of the deposits are brown to yellowish brown and vary among 7.5YR4/4, 10YR4/3 and 10YR4/4. The heavy mineral composition is dominated by intact pyroxene group and amphibole group minerals, which are very susceptible to chemical weathering, thus indicating the unweathered character of the deposits. Epidote group minerals are the third important fraction. The three mineral groups, which amount to more than 80%, originate mainly from local metamorphic rocks. Some orthopyroxenes and brown hornblendes are derived from the Etendeka volcanics in the upper Hoanib catchment. Carbonate contents of 4.3–12.4% are typical of a dry environment. They may well be due to aeolian input, as dust storms transporting calcareous particles are very common for the region (Eitel, 1994; Tyson et al., 2002), and/or caused by fluvial erosion of lime bearing Damara schists and dolomites in the middle section of the Hoanib river course (e.g., Khowarib gorge marbles and dolomites).

X-ray diffraction patterns of the clay fraction exhibit a dominance of illite and chlorite. Only sample 2/4 from Amspoort contains an appreciable amount of smectite. Nonoblique illite peaks indicate fresh and unweathered particles. Authigenic or reworked palygorskite, often associated with secondary carbonate or calcretes (Eitel, 1993, 2000), could not be detected.

At locality 1, the Amspoort Silt terrace is only about 3 m thick. Silty deposits prevail only in the central part of the complex. Following the fluvial deposition of sandy and silty sediments, aeolian sands buried the fluvial sequence. At locality 2, the Amspoort Silts reach their maximum thickness. Here, silty sediments dominate the ~14-m-thick deposits. The upper silty complex contains more pyroxene group minerals than the layers below indicating different source areas. Locality 3 is situated at the upstream end of the Amspoort terrace. As at locality 1, the deposits have a total thickness of only 2–3 m.

4.2. Chronometry

4.2.1. ^{14}C dating

Table 1 shows the results from the radiocarbon analyses. The data confirm that the wood was buried by a Late Holocene accumulation of the Amspoort Silts. The compiled radiocarbon data of in situ trees originate from Rust (1999) and our own investigations (all data calibrated according to Stuiver et al., 1998). The spatial distribution of the ^{14}C samples is shown in Fig. 6.

4.2.2. OSL dating

Results of luminescence dating are given in Tables 2 and 3. Low-level γ-spectrometry indicates slight radioactive disequilibrium for sample HDS-1269 (Table 2), which is taken into account in the age calculation. While almost all measured aliquots proved to be free of feldspar, five aliquots of sample HDS-1267 showed minor feldspar contamination, however with very low IR-stimulated luminescence signals of only <1% of the B-OSL signal.

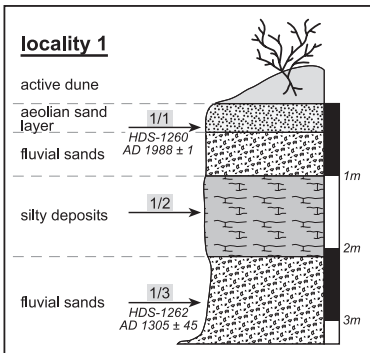

No.	colour	carbonate	particle size fractions [%] >2mm	sand	silt	clay	heavy minerals [%] ep	pyr	hbl	z.r.t.	others	clay minerals illite	chlorite	smectite	palygorskite
1/1	7.5 YR 4/4	4.3 %	0	83	11	6	50	14	22	5.5	8.5	+++	+	–	–
1/2	10 YR 4/4	12.4 %	0	4	62	34	24	44	22.5	5	4.5	+++	+	–	–
1/3	7.5 YR 4/4	4.7 %	0	90	7	3	29	40	24	5	2	+++	+	–	–

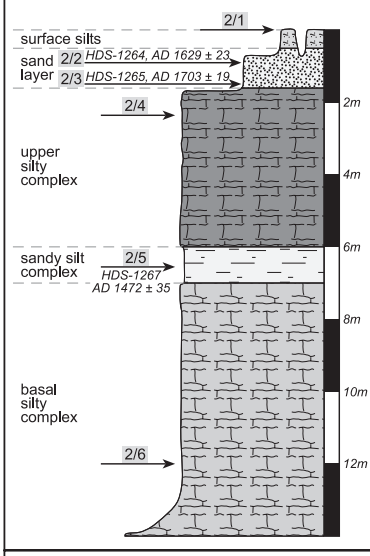

No.	colour	carbonate	particle size fractions [%] >2mm	sand	silt	clay	heavy minerals [%] ep	pyr	hbl	z.r.t.	others	clay minerals illite	chlorite	smectite	palygorskite
2/1	10 YR 4/4	7.4 %	0	7	80	13	26	45	19	6	4	+++	+	–	–
2/2	7.5 YR 4/4	5.5 %	0	62	32	6	20	47	20	2	11	+++	+	–	–
2/3	7.5 YR 4/4	4.2 %	0	94	4	2	31	49	12	6	2	+++	+	–	–
2/4	10 YR 4/3	12.4 %	0	2	55	43	29	23	42	3	3	+++	+	+	–
2/5	10 YR 4/4	5.8 %	0	35	56	9	23	33	27	4	13	+++	+	–	–
2/6	10 YR 4/4	11.0 %	0	8	75	17	37	25	30	2	6	+++	+	+	–

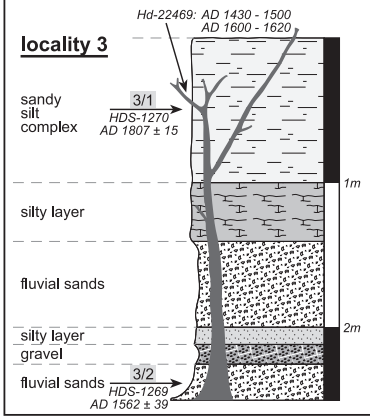

No.	colour	carbonate	particle size fractions [%] >2mm	sand	silt	clay	heavy minerals [%] ep	pyr	hbl	z.r.t.	others	clay minerals illite	chlorite	smectite	palygorskite
3/1	10 YR 4/3	7.6 %	0	41	47	12	30	35	29	2	4	+++	+	–	–
3/2	10 YR 4/4	5.5 %	0	60	35	5	29	23	42	3	3	+++	+	–	–

Design: V. Schniepp

Fig. 5. Sedimentological characteristics and OSL chronometry of the Amspoort Silt terrace deposits downstream of (locality 1), near (locality 2) and upstream of Amspoort (locality 3) (see Fig. 6). Hd-22469 in locality 3 represents calibrated radiocarbon ages BP (=before 1950) (see Table 1).

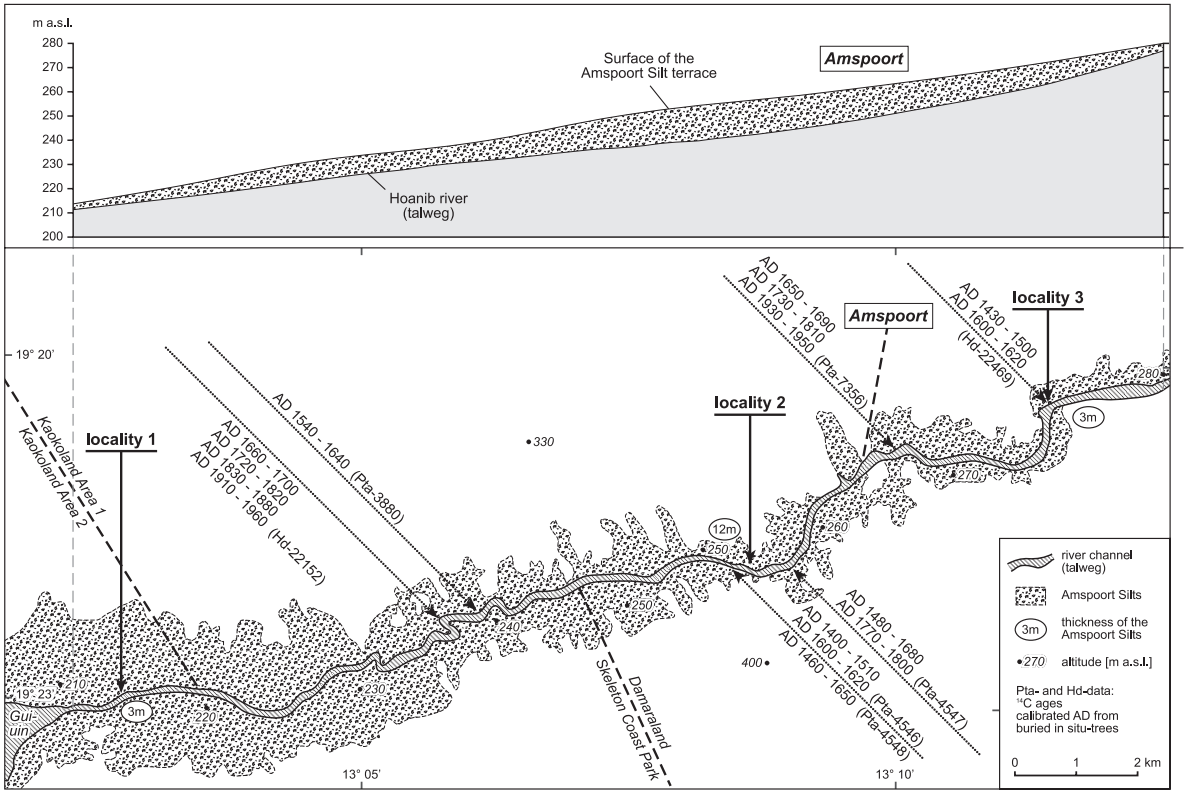

Fig. 6. Thickness and extension of the Amspoort Silt terrace along the lower Hoanib valley with $^{14}C_{cal}$ data (2σ-error, see Table 1) of buried in situ trees (graph based on the topographical map of Namibia, sheet no. 1913AC Amspoort, scale 1:50,000.). The figure illustrates the sedimentation of the deposits in a distinct and narrow valley section. This situation disagrees with conditions forming floodouts as assumed by Heine (2004).

Steep shine-down curves with several 10^3–10^4 counts during the first 0.4 s reach the background level after only 2–3 s of optical stimulation (Fig. 7a). The samples show hardly any recuperation of the luminescence signal and usually exhibit an excellent reproduceability of the twice measured lowest regeneration dose point (Fig. 7b, results of twice measured dose point were almost indistinguishable). The few aliquots exhibiting a reproduceability >10% were exluded from D_E-value data sets.

Dose recovery measurements reveal high precision and correctness of the data gained with the applied

Table 2
Dose rate data of the Amspoort Silts OSL samples

Lab. no.	Locality/ sample no.	Depth b.g.l. (m)	Uranium (μg/g)	Thorium (μg/g)	Potassium (wt.%)	Effective dose rate (Gy/ka)
HDS-1260	1/1	0.3	1.65±0.07	7.33±0.14	1.79±0.05	2.71±0.15
HDS-1262	1/2	2.6	1.74±0.08	7.35±0.28	1.69±0.08	2.62±0.16
HDS-1264	2/2	0.4	2.09±0.05	7.87±0.11	1.59±0.04	2.66±0.15
HDS-1265	2/3	1.5	1.72±0.08	7.72±0.27	1.84±0.09	2.79±0.17
HDS-1267	2/5	7.0	2.22±0.10	7.98±0.29	1.80±0.09	2.83±0.17
HDS-1269	3/2	2.3	2.07±0.05[a]	8.45±0.14	1.65±0.04	2.73±0.15
HDS-1270	3/1	0.4	2.07±0.05	7.97±0.11	1.63±0.04	2.70±0.15

[a] Sample showing radioactive disequilibrium in ^{238}U-chain, as detected by low-level gamma-spectrometry.

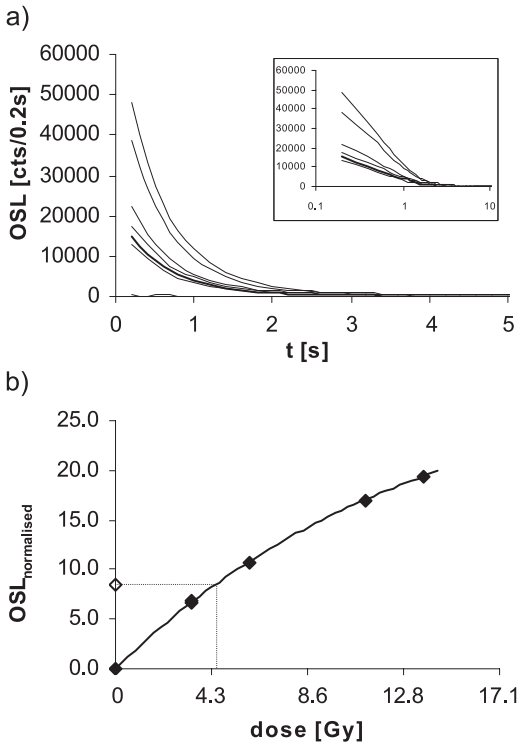

Fig. 7. Typical example of shine-down curves (a) and growth curves (b) represented by an aliquot of sample HDS-1267. Shine downs delivering several 10^3–10^4 counts in the most light-sensitive initial integral reach the background level after only 2–3 s of blue stimulation (cf. also inlet with logarithmic time axis). Most of the measurements exhibit excellent reproduceabilities of the lowest dose point of <10% (here: 0.97) and small recuperation of the luminescence signal (here: 0.67%).

SAR technique. For all samples the laboratory doses were met within the 2-σ-standard deviation of the mean dose value (cf. Table 3). This finding also indicates that the studied samples do not show any malign signs of thermal transfer caused by preheating as reported by Rhodes (2000) and Roberts et al. (2000). The coefficient of variation v (i.e., standard deviation/mean×100) of the artificially bleached samples ranges between 3.9% and 9.8%.

For the D_E-value distributions of the natural samples, however, v ranges between 7.2% (HDS-1269) and >100%. (In order not to artificially restrict v, the D_E-values that had to be extrapolated beyond the highest dose point were also considered.) Apart from sample HDS-1269 v lies above the threshold value of 10% usually considered as acceptible for sufficiently bleached sediments (Fuchs and Wagner, 2003). Even the aeolian transported sample HDS-1260 possesses a v-value of 22%, clearly indicating insufficient zeroing of the luminescence signal prior to deposition. (In the field, care was of course taken care not to sample obviously bioturbated or otherwise disturbed material, which might exhibit similarly widely spreaded D_E-distributions as differentially bleached sediments). Again with the exception of sample HDS-1269, v-values of the natural samples are also much higher than the ones found for the artificially zeroed samples. Additionally, insufficient bleaching of the samples is well illustrated by Fig. 8, in which D_E-values of single aliquots are plotted against the normalised natural luminescence signal of the measured aliquots, as suggested by Li (1994) and Clarke (1996). Although it exhibits a much smaller scatter than the other samples, sample HDS-1269 also shows a positive correlation between the size of the D_E-values and the strength of the (normalised) luminescence signals.

Apparently, insufficient bleaching of sediments is not unusual for the northern Namib Desert. One out of seven OSL samples dated from the Khumib river catchment and 7 out of 11 samples collected from the nearby Hoarusib valley display beyond-threshold v-values of 18% and up to 26%, respectively (Srivastava et al., 2004a,in press), although the problem of insufficient bleaching is not adressed by the authors. On the contrary, in both cases, the authors explicitly assume that the desert environmment guarantees a proper zeroing of the luminescence signal.

In the present study, OSL age calculation was based on the lower edge of the gained D_E distributions. D_E-values of the natural samples were sorted in ascending order and a mean D_E-value was calculated from the lower edge showing a similar v-value as the artificially bleached samples. The standard error was used for age calculation. Since for sample HDS-1264 the standard deviation even of the two lowest gained D_E-values of the natural sample is higher than the one of all the artificially bleached aliquots, the lowest paleodose produced by the SAR protocol was considered for age determination.

Thus, apart from sample HDS-1269, the calculated OSL ages are strictly speaking maximum ages.

As Wallinga (2002) has pointed out, D_E-value scatter may be erroneously high not only in really

Table 3
Dose data (artificially bleached samples), palaeodose data (natural samples) and OSL ages of the Amspoort Silt samples

Lab. no.	Artificially dosed aliquots			Aliquots with natural luminescence signal						
	Applied D_E (s)[a]	Recovered D_E with standard deviation and v [a](s)[a]	(%)	D_{Emean} with standard deviation and v[b] (Gy)	(%)	D_{Emin} with standard error, v and N[c] (Gy)	(%)	$N_{of\ 32}$	Age/maximum ages derived from D_{Emin} (a)	AD
HDS-1260	1	1.08±0.11	9.8	0.06±0.01	22.0	0.04±0.002	5.7	2	≤13±1	≥1988±1
HDS-1262	28	28.02±2.13	7.6	3.74±5.55	148.4	1.82±0.13	7.1	7	≤696±45	≥1305±45
HDS-1264	21	21.96±0.85	3.9	3.85±4.39	114.0	0.99–	–	1	≤372±23	≥1629±25
HDS-1265	18	18.14±0.83	4.6	2.61±3.16	120.8	0.83±0.03	4.1	5	≤298±19	≥1703±19
HDS-1267	24	23.54±1.90	8.1	2.27±1.08	47.7	1.50±0.12	8.1	11	≤529±35	≥1472±35
HDS-1269	13	12.34±0.80	6.5	1.17±0.08	7.2	1.16±0.07	6.4	30	439±39	≥1562±39
HDS-1270	20	19.92±1.89	9.5	1.95±2.60	133.1	0.52±0.04	8.1	2	≤194±15	≥1807±15

[a] The calibration source within the used Riso-TL/OSL-reader DA15 has a current dose rate of ~5.1 Gy/min.
[b] Including also D_E -values which had to be extrapolated above the highest applied regeneration dose point.
[c] D_{Emin} was extracted from the lower edge of the D_E distribution, which exhibits a threshold v-value similar (i.e., ≤) to those of the artificially dosed aliquots.

badly bleached sediments, clearly overestimating the true paleodose, but also in samples with a low content of insufficiently bleached grains. OSL calculation from the lower edge of samples which are only moderately contaminated by insufficiently bleached sediment grains may even lead to the true age value, if contamination does not exceed ~5%. Yet, unless single grain analyses are carried out, there is no direct control of the true degree of contamination with improperly zeroed material. Apart from the well-bleached sample, HDS-1269 and the aeolian sample HDS-1260, D_E distributions are positively skewed (cf. Fig. 8). As Olley et al. (1999) have pointed out, dose distributions from small aliquots will only be strongly asymmetric at contamination levels <5%. However, for the present study stratigraphic and independent age control may also serve as indications of how well the maximum OSL ages present the true ages of the sediment deposition.

- At all three localities, OSL ages are stratigraphically consistent, increasing in age with depth.
- At locality 2, the OSL ages of sample HDS-1265 and HDS-1264, taken from the same sand layer produce OSL ages of ≤298±19 and ≤372±23 a which are identical within the 2σ-error level (although sample HDS-1264 seems to be the worst bleached sample!)
- At locality 3, sample HDS-1269 yields a date of AD 1562±39 for the basal fluvial sands, which is in agreement with the ^{14}C date of AD 1430–1500/1600–1620 (Hd-22469, 2σ-error level), calculated for the tree buried by the Amspoort Silt formation.
- The age of AD ≤1472±35 gained for the lowest dated OSL sample at locality 2 (HDS-1267) is in agreement with two ^{14}C dates of AD 1400–1510/1600–1620 (Pta-4546, 2σ-error level) and AD 1460–1650 (Pta-4548, 2σ-error level) of in situ tree-wood samples collected by Rust (1999) just on the opposite side of the same river bend.
- At locality 1, sample HDS-1260 delivers a very young age for the aeolian sandy layer deposited on the underlying fluvial sediment complex. If OSL ages are calculated for the single aliquots, apparent ages range from 13 to 32 years. Although the sample shows a v-value of 22%, clearly indicating insufficient bleaching, the remnant dose is neglectible. This example clearly supports the findings of Wallinga (2002) that insufficient bleaching might be best detectible in less (to almost not) insufficiently bleached samples.

From these observations we conclude that the maximum OSL ages gained from the lower edge of the D_E-value distributions may rather be considered as semitrue ages.

5. Interpretation

The Amspoort Silt formation is made of river-end deposits caused by an aridification during the Late

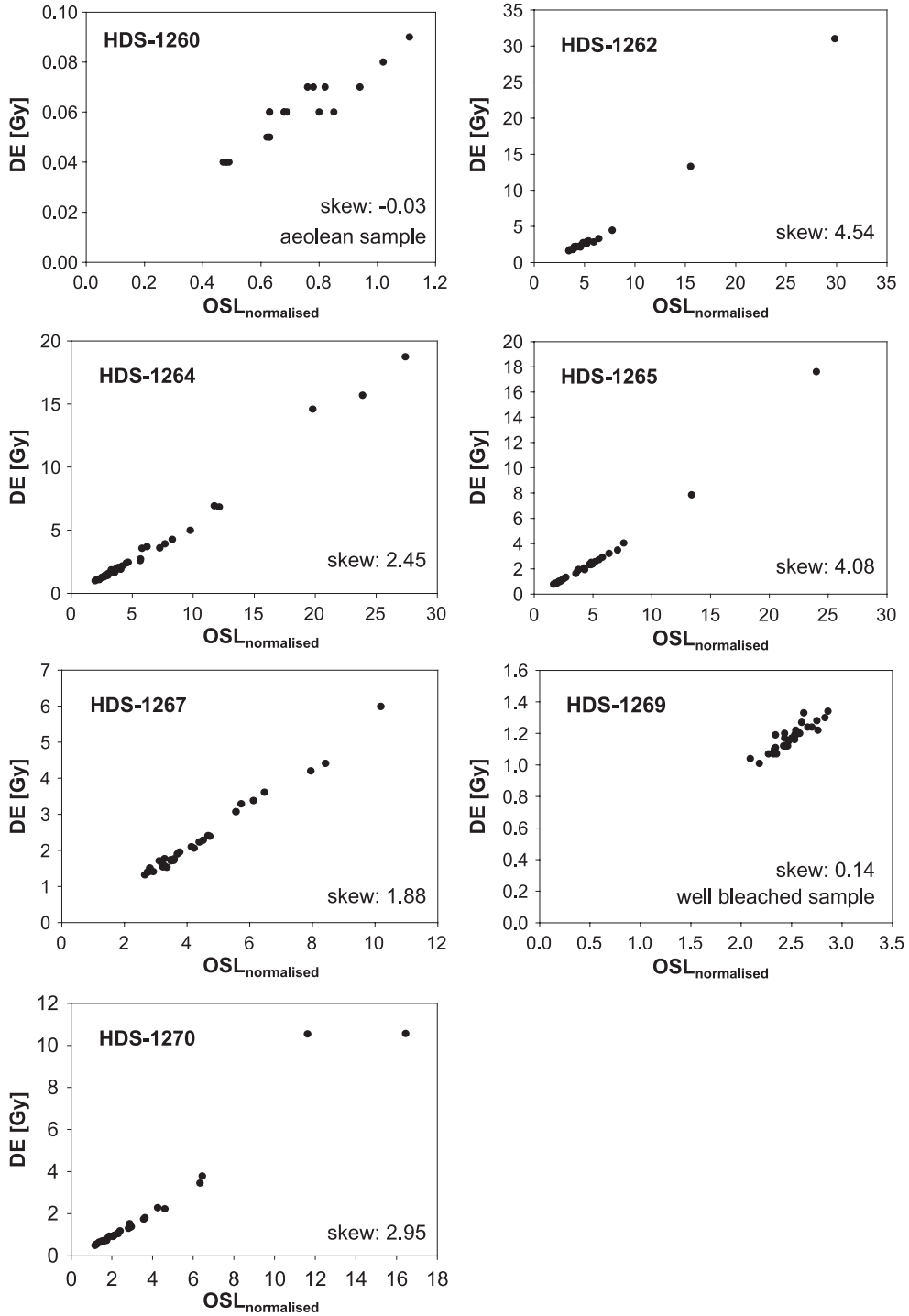

Fig. 8. D_E-values versus normalised luminescence intensity. D_E-value scatter shows a strong dependency on the (normalised) luminescence intensity indicating a poor bleaching of the sediments.

Holocene. This is concluded from the apparent upstream shift of the main sedimentation area over time during the drying period. The earliest sedimentation was detected at the downstream position of locality 1. Here, the central silty deposits above the basal fluvial sands give evidence of a low energy runoff regime of the ending Hoanib river. The OSL data suggest that ~10 km downstream of Amspoort the filling of the valley with fine-grained material started after AD 1305 (≤696±45 a). The deposition of the basal fluvial sands occurred during the preceding wet period. The silt complex is covered by 1.1-m-thick layer of little consolidated fluvial and aeolian sands, that give an rather young OSL date of ≤13±1 a.

Further upstream, the silty deposits become much thicker. In the middle part of the Amspoort Silt terrace, the well stratified sediments fill the valley with a total thickness of ~14 m. At locality 2 the basal silt complex is covered by a more sandy layer (sample 2/5) that formed after AD 1472 (≤529±35 a). Above the upper silt complex, sandy deposits formed approximately 300 years ago (≤298±19 and ≤372±23 a).

Locality 3 is typical of the upstream end of the Amspoort Silts. Instead of a thick silty complex, only 1.4 m of fine-grained silty deposits are found on top of a sequence of fluvial sands, silts and gravels. The basal coarse layers formed when the river ended further downstream (AD 1562; 439±39 a). As sample HDS-1269, which delivers the OSL age for the basal sediments, does not exhibit any sign of insufficient bleaching, the date is certainly no maximum age but a reliable age of deposition. The silt complex of the upper 1 m are the youngest sediments of the whole Amspoort Silt terrace, which formed in the 19th century (≤194±15 a).

In the 14th century the Hoanib river was still depositing sandy material indicating wet conditions. Between the 15th century and the 19th century, the Hoanib river became shorter with the major sedimentation area shifting upstream. River shortening was caused by decreased runoff due to increasing aridification in the river catchment. For the longest time the river ended near Amspoort, where it deposited alone ~7 m of fine-grained material beween the 15th and 17th/18th century. Aridification of the highlands in northwestern Namibia culminated in the 18th/19th century when the river ended already east of Amspoort.

After the deposition of the youngest sediments in the 19th century (sample HDS-1270, ≤194±15 a) runoff must have increased due to intensified rainfall in the catchment area, because the river has incised deeply into the Little Ice Age deposits, reexposing the buried riverine forest.

At first glance, the radiocarbon data in Fig. 6 do not seem to support an upstream shift of the sedimentation sink during the Little Ice Age period. In this respect, two complicating aspects of ^{14}C dating have to be considered. First, radiocarbon dates from wood that is only some hundreds of years old are difficult to calibrate (e.g., Stuiver et al., 1998). Error ranges are wide because of changing ^{14}C contents in the palaeoatmosphere. Second, another uncertainty derives from the fact that trees which become embedded might survive and even grow for an unknown period. Our observations in the area show that trees (esp. *Acacia* sp.) can survive even if they are buried by aeolian sands up to more than 1.5 m. Prolonged growth during embedding seems to be especially likely for sample Hd-22152, which, according to ^{14}C dating, did not die any earlier than in the 17th century, while sample Pta-3880 collected only some hundreds of metres upstream, may have stopped photosynthesis as early as the 16th or even the 15th century. However, the ^{14}C data confirm deposition of the Amspoort Silts during the Little Ice Age. Opposite locality 2, samples Pta-4546 and Pta-4548 both deliver unambiguous dates with rather narrow error ranges. As the data state that the two sampled trees did not die earlier than in the 15th century, respectively, they indicate that the basal silty complex at locality 2 is probably not significantly older than the OSL-dated sandy silt complex deposited AD ≤1472±35.

According to Rust (1999), present-day river-end depositioning occurs at the flood basin of the Gui-uin (Figs. 1 and 9). As the reservoir is dammed by the Skeleton Coast dune belt, sedimentation is at least partly due to dune damming (Krapf et al., 2002; Svendsen et al., 2003, personal field observations in September 2001 and pers. comm. J. Paterson/Nature Conservation Möwebaai). Thicker deposits cannot form, because the Hoanib breaks through the Skeleton sand field every 5–7 years, thus eroding formerly

Fig. 9. NE-oriented view onto the Gui-uin flood plain downstream of Amspoort. The photo shows approximately 1-m-thick silty alluvial material deposited at the southern margin of the Gui-uin flood plain during the austral summer 1999/2000.

sedimented silty material and carrying it into the erg and into the ocean (Blümel et al., 2000; Svendsen et al., 2003).

6. Conclusion

OSL analyses prove to be a valuable dating tool for desert-margin river-end deposits. In the Amspoort study area, it delivers sufficient time resolution to trace spatial shifts of former aggradation processes along the Hoanib talweg during the Little Ice Age period. Apart from the chronometry, the data help to clarify a controversial discussion on the Amspoort Silt formation.

The data confirm that the Amspoort Silts are river-end deposits sensu Rust (1999). This may be deduced from the observed upstream shift of the main sedimentation sink during the dry Little Ice Age period. The Amspoort Silts are not floodout sediments (Tooth, 1999) as suggested by Heine and Heine (2002: p. 124), because high-energy floodouts change into low-energy flows when they leave a gorge or a narrow valley and spread over a large area. They are also not slackwater deposits (Heine, 2004; Srivastava et al., in press) that formed in the backwaters of large floods. In contrast to these suggestions, (I) the Amspoort Silts accumulated inside the narrow Hoanib valley fixed by steep slopes on both sides, (II) they are well-laminated sediments of low-energy flows without any coarse pebbles or boulders indicating high floods, (III) they were deposited in the central valley sections and not as backfood deposits behind big rocks or in protected environs of the mouths of tributaries, (IV) they occur in a well-defined part of the valley course with an upper and lower endpoint (Fig. 6) and (V) sedimentation ages show an upstream shift of the sedimentation area due to aridification of the river catchment area. Additionally, we can also exclude silt accumulation by dune damming because the surface of the silt terrace is not horizontal but follows the inclination of the valley bottom.

River-end deposits are very well suited to provide evidence of hydrological fluctuations and dry conditions in the hinterland. The sediments are excellent objects to reconstruct past climatic fluctuations at desert margins. This should be taken as a forthcoming challenge, as for desert margin areas there are only a small number of proxies available, which indicate regional precipitation changes.

In the northern hemisphere, the Little Ice Age culminated in the 18th and early 19th century with the lowest temperatures during the past 1000 years (Bradley et al., 2003). The Amspoort Silt terrace shows that this period was characterized by decreased rainfall in northern Namibia. This finding contributes to the discussion of whether and where global cooling correlates with aridification, or whether and where

global warming is related to increased precipitation caused by a higher water content of the atmosphere. Present-day erosion of the Amspoort Silt evidences increased rainfall and relatively high runoff of the Hoanib River. This is in contrast to the hypothesis of a natural aridification of southwestern Africa since the Little Ice Age (Walter, 1954) or since Colonial times (Ward and Ngairorue, 2000), respectively. Nevertheless, large parts of the northern highlands of Namibia are characterized by aridification. Thus, actual erosion of the Amspoort silts confirms the results of sedimentological and pedological studies carried out in the semiarid highland savannas of Namibia, which state that the observed environmental changes are most likely caused by human impact and desertification processes (Brunotte et al., 2002; Eitel et al., 2002b), not by climatic change.

Acknowledgement

As part of the geomorphological project 'Hygric fluctuations in northwestern Namibia' and connected with the IGCP 413 on dryland environmental changes, the study was generously supported by the German Science Foundation (Deutsche Forschungsgemeinschaft, DFG). We thank Nature Conservation Namibia for the permission to work in the Skeleton Coast Park, and Mr. John Paterson, Möwebaai for his friendly support. We would like to thank D.S.G. Thomas, Oxford/UK, and I. Livingstone, Northhampton/UK, for their critical comments, S. Lindauer and A. Al-Karghuli for their assistance in the laboratory, and E. Roberts and K. Carriere, who helped to improve the English. This paper is dedicated to Uwe Rust, Ludwig-Maximilians-University München/Germany, who was the first geomorphologist to study and compare in detail river silt deposits in northwestern Namibia during the 1970s and 1980s.

References

Blümel, W.D., Hüser, K., Eitel, B., 2000. Uniab-Schwemmfächer und Skelettküsten-Erg: Zusammenspiel von äolischer und fluvialer Dynamik in der nördlichen Namib. Regensburger Geographische Schriften 33, 37–56.

Boenigk, W., 1983. Schwermineralanalyse. Enke, Stuttgart.

Bøtter-Jensen, L., 1997. Luminescence techniques: instrumentation and methods. Radiation Measurements 27, 749–768.

Bradley, R.S., Briffa, K.R., Cole, J., Osborne, M.K., 2003. The climate of the last millenium. In: Alverson, K.D., Bradley, R.S., Pedersen, T.F. (Eds.), Paleoclimate, Global Change and the Future. Springer, Berlin, pp. 105–141.

Brunotte, E., Sander, H., Frangen, J., 2002. Human-induced environmental changes in areas favorable and unfavorable for land-use in Kaokoland, Namibia. Die Erde 133, 133–152.

Clarke, M.L., 1996. IRSl dating of sands: bleaching characteristics at deposition inferred from the use of single aliquots. Radiation Measurements 26, 611–620.

Eitel, B., 1993. Kalkkrustengenerationen in Namibia: Carbonatherkunft und genetische Beziehungen. Die Erde 124, 85–104.

Eitel, B., 1994. Kalkreiche Decksedimente und Kalkkrustengenerationen in Namibia: Zur Frage der Herkunft und Mobilisierung des Calciumcarbonats. Stuttgarter geographische Studien vol. 123. Geographisches Institut, Stuttgart, 193 pp.

Eitel, B., 2000. Different amounts of palygorskite in South West African Cenozoic calcretes: geomorphological, paleoclimatological and methodological implications. Zeitschrift für Geomorphologie NF Supplementband 121, 139–149.

Eitel, B., Blümel, W.D., Hüser, K., Mauz, B., 2001. Dust and loessic alluvial deposits in Northwestern Namibia (Damaraland, Kaokoveld): sedimentology and palaeoclimatic evidence based on luminescence data. Quaternary International 76/77, 57–65.

Eitel, B., Blümel, W.D., Hüser, K., 2002a. Environmental transitions between 22 ka and 8 ka in monsoonally influenced Namibia—a preliminary chronology. Zeitschrift für Geomorphologie NF Supplementband 126, 31–57.

Eitel, B., Eberle, J., Kuhn, R., 2002b. Holocene environmental change in the Otjiwarongo thornbush savanna (Northern Namibia): evidence from soils and sediments. Catena 47, 43–62.

Fuchs, M., Wagner, G.A., 2003. Recognition of insufficient bleaching by small aliquots of quartz for reconstructing soil erosion in Greece. Quaternary Science Reviews 22, 1161–1167.

Heine, K., 2004. Little Ice Age climatic fluctuations in the Namib Desert, Namibia, and adjacent areas: evidence of exceptionally large floods from slack water deposits and desert soil sequences. Lecture Notes in Earth Sciences 102, 137–165.

Heine, K., Heine, J.T., 2002. A palaeohydrologic reinterpretation of the Homeb silts, Kuiseb River, Central Namib Desert (Namibia) and paleoclimatic implications. Catena 48, 107–130.

Heine, K., Heine, C., Kühn, Th., 2000. Slackwater Deposits in der Namib-Wüste (Namibia) und ihr paläoklimatischer Aussagewert. Zentralblatt für Geologie und Paläontologie, Teil 1: Allgemeine, Angewandte, Regionale und Historische Geologie 1999 (5/6), 587–613.

Krapf, C., Stollhofen, H., Stainistreet, I., 2002. Contrasting Styles of Ephemeral River Systems and their Interaction with Dunes of the skeleton Coast Erg-NW Namibia Poster displayed at the Dryland Rivers Conference, Process and Product, Aberdeen, Scotland: 8–9 August, 2002.

Kretzschmar, R., 1996. Kuturtechnisch-bodenkundliches Praktikum, Ausgewählte Laborund Feldmethoden, vol. 1. University of Kiel, Germany. 503 pp.

Li, S.-H., 1994. Optical dating: insufficiently bleached sediments. Radiation Measurements 23, 563–567.

Marker, M.E., 1977. Aspects of the geomorphology of the Kuiseb River, South West Africa. Madoqua 10, 199–206.

Murray, A.S., Wintle, A.G., 2000. Luminescence dating of quartz using an improved single-aliquot regenerative-dose protocol. Radiation Measurements 32, 57–73.

Olley, J., Caitcheon, G., Murray, A., 1998. The distribution of apparent dose determined by optically stimulated luminescence in small aliquots of fluvial quartz: implications for dating young sediments. Quaternary Geochronology 17, 1033–1040.

Olley, J.M., Caitcheon, G.G., Roberts, R.G., 1999. The origin of dose distribution in fluvial sediments, and the prospect of dating single grains from fluvial deposits using optically stimulated luminescence. Radiation Measurements 30, 207–217.

Prescott, J.R., Hutton, J.T., 1998. Cosmic ray and gamma ray dosimetry for TL and ESR. Nuclear Tracks and Radiation Measurements 14, 223–227.

Rhodes, E.J., 2000. Observations of thermal transfer OSL signals in glacigenic quartz. Radiation Measurements 32, 595–602.

Roberts, R.G., Galbraith, R.F., Yoshida, H., Laslett, G.M., Olley, J.M., 2000. Distinguishing dose populations in sediment mixtures: a test of single-grain optical dating procedures using mixtures of laboratory-dosed quartz. Radiation Measurements 32, 459–465.

Rust, U., 1987. Geomorphologische Forschungen im südwestafri kanischen Kaokoveld zum angeblichen vollariden quartären Kernraum der Namibwüste. Erdkunde 41, 118–133.

Rust, U., 1989. (Paläo)- Klima und Relief: Das Reliefgefüge der südwestafrikanischen Namibwüste (Kunenz bis 27° s Br.). Münchner Geographische Abhandlungen 7 (158 pp.).

Rust, U., 1999. River-end deposits along the Hoanib-River, northern Namib: archives of Late Holocene climatic variation on a subregional scale. South African Journal of Science 95, 205–208.

Rust, U., Vogel, J.C., 1988. Late Quaternary environmental changes in the Namib Desert as evidenced by fluvial landforms. Palaeoecology of Africa 19, 127–137.

Rust, U., Wieneke, F., 1974. Studies on gramadulla formation in the middle part of the Kuiseb River, South West Africa. Madoqua II/3, 3–15.

Schilles, Th., 1998. Entwicklung und Anwendung einer Technik zur 'Single Aliquot' Datierung mittels optisch stimulierter Lumineszenz. Diplomarbeit Fakultät für Physik und Astronomie der Universität Heidelberg. 81 pp.

Spönemann, J., Brunotte, E., 2002. In: Pörtge, K.H. (Ed.), Paläozoische Talsysteme in Namibia: Morphogenetische Widersprüche und morphotektonische Aspekte. Afrikagruppe deutscher Geowissenschaftler (AdG), Göttingen.

Srivastava, P., Brook, G.A., Marais, E., 2004a. A record of fluvial aggradation in the northern Namib Desert margin during the Late Pleistocene-Holocene. Zeitschrift für Geomorphologie NF Supplementband 133, 1–18.

Srivastava, P., Brook, G.A., Marais, E., 2004b. Luminescence chronology and depositional environment of the Hoarusib River Clay Castle sediments, northern Namib Desert, Namibia. Catena (in press).

Stuiver, M., Reimer, P.J., Bard, E., Beek, J.W., Burr, G.S., Hughen, K.A., Kromer, B., McCormae, F.G., van der Plicht, J., Spurk, M., 1998. INTCAL 98 Radiocarbon age calibration, 24, 000-0 cal BP. Radiocarbon 40, 1041–1083.

Svendsen, J., Stollhofen, H., Krapf, C.B.E., Stanistreet, I.G., 2003. Mass and hyperconcentrated flow deposits record, dune damming and catastrophic breakthrough of ephemeral rivers, Skeleton Coast Erg, Namibia. Sedimentary Geology 160, 7–31.

Tooth, S., 1999. Floodouts in Central Australia. In: Miller, A.J., Gupta, A. (Eds.), Varieties in Fluvial Forms. Wiley, Chichester, pp. 219–247.

Tyson, P., Odada, E., Schulze, R., Vogel, C., 2002. Regional-global change linkages: Southern Africa. Global-Regional Linkages in the Earth System IGBP Global Change. Springer, Heidelberg, pp. 3–73.

Velde, B., 1995. Composition and origin of clays. In: Velde, B. (Ed.), Origin and Mineralogy of Clays, Clays and Environment. Springer, Berlin, pp. 8–42.

Vogel, J.C., 1989. Evidence of past climatic change in the Namib Desert. Palaeogeography, Palaeoclimatology, Palaeoecology 70, 355–366.

Vogel, J.C., Rust, U., 1990. Ein in der kleinen Eiszeit (Little Ice Age) begrabener Wald in der nördlichen Namib. Berliner Geographische Studien 30, 15–34.

Wallinga, J., 2002. On the detection of OSL age overestimation using single-aliquot techniques. Geochronometria—Journal on Methods and Applications of Absolute Chronology 21, 17–26.

Walter, H., 1954. Teil I: Grundlagen der Weidewirtschaft in Südwestafrika. In: Walter, H., Volk, O.H. (Eds.), Grundlagen der Weidewirtschaft in Südwestafrika. Ulmer, Stuttgart, pp. 1–182.

Ward, D., Ngairorue, B.T., 2000. Are Namibia's grasslands desertifying? Journal of Range Management 53/2, 138–144.

Zawada, P.K., 1997. Palaeoflood hydrology: method and application in flood-prone southern Africa. South African Journal of Science 93, 111–132.